Solutions to Problems Chapter 2

l. Assume a Gaussian beam in air with plane wavefronts and waist w_0 at a distance d_0 from a converging lens of focal length f .

(a) Using the laws of q-transformation, find the distance behind the lens where the Gaussian beam focuses, i.e., again has plane wavefronts.

(b) Using the beam propagation method, simulate the propagation of the beam through air and through a lens.

(c) By setting $d_0 = f$, determine the profile of the beam a distance f behind the lens.

(d) By setting $d_0 = 2f$, determine the profile of the beam distances f and $2f$ behind the lens.

A1. (a) Using laws of q-transformation, the q after the lens and after a distance of propagation z is $q(z) = \dfrac{f(q_0 + d_0)}{f-(q_0+d_0)} + z$, $q_0 = jz_R = jk_0 w_0^2/2$. So $q(z) = f\dfrac{[d_0(f-d_0) - z_R^2] + jz_R f}{(f-d_0)^2 + z_R^2)} + z$.

When the Gaussian beam focuses, its q becomes purely imaginary again; hence its real part becomes equal to zero. Using the above relations, this occurs at $z = \dfrac{f(z_R^2 + d_0^2 - fd_0)}{(f-d_0)^2 + z_R^2}$. The imaginary part yields the new beam waist with a Raleigh range $z_R' = \dfrac{f^2 z_R}{(f-d_0)^2 + z_R^2}$.

(b) Assume initial Gaussian beam with $w_0 = 0.1mm$, wavelength $\lambda = 0.5\mu m$.

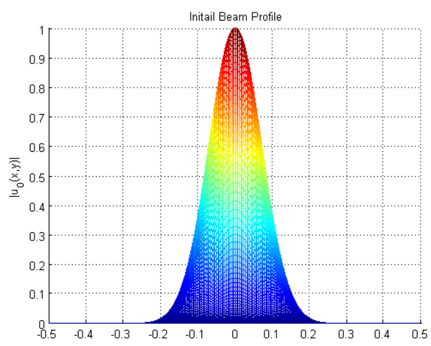

Beam propagates by the Rayleigh range $z_R = 63.8mm = f$, the focal length of the lens.

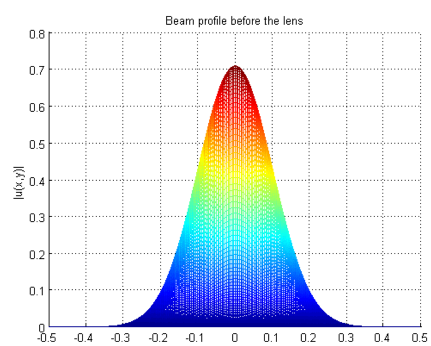

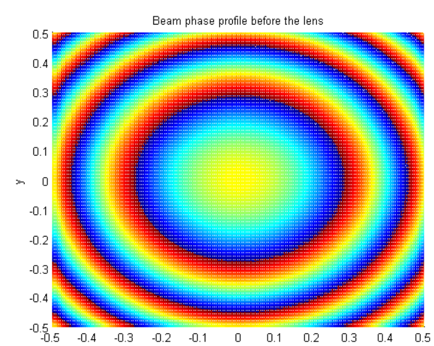

Immediately after lens, the phase should be equal in magnitude to the incident phase but opposite in sign.

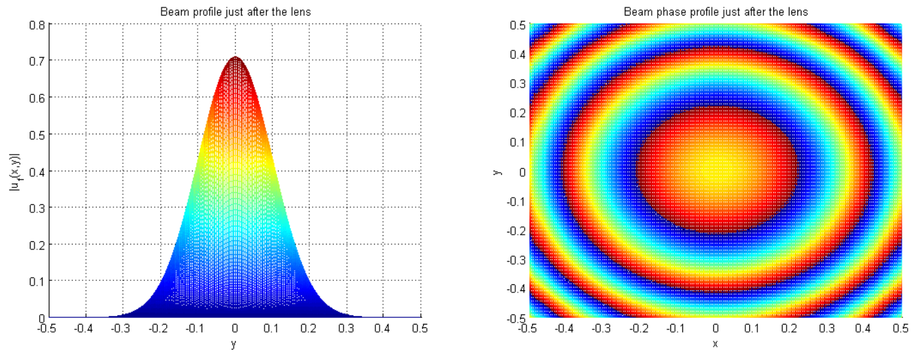

At back focal plane of lens, the initial Gaussian beam with plane is retrieved. Some residual phase remains due to numerical errors.

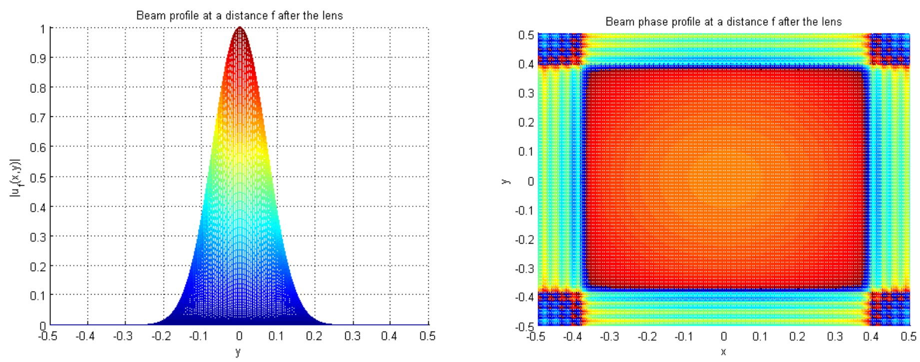

After further travel from back focal plane by distance *f*, the beam again diverges as shown.

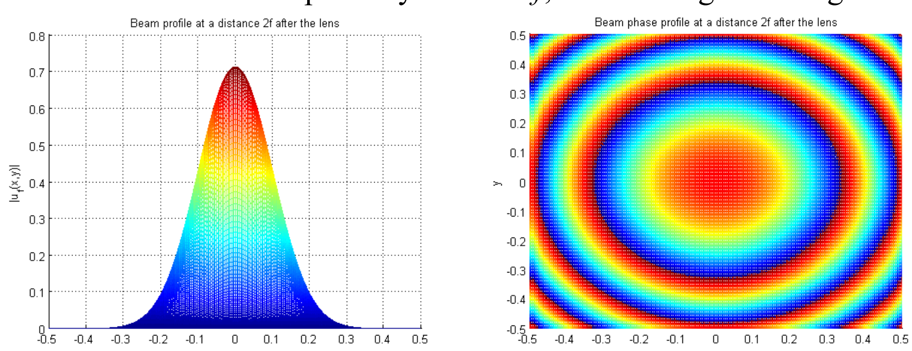

(c) If $d_0 = f$, then it follows from the expression of $q(z)$ in part (a) that at $z = f$, the Gaussian beam again attains plane wavefronts and hence a waist at the back focal plane. Here, $z_R' = \dfrac{f^2}{z_R}$.

Also, for the final waist to be the same as the initial waist, $z_R = f$, i.e., the Rayleigh range of the initial Gaussian beam should be the same as the focal length of the lens.

(d) Again, using the expression for $q(z)$ in part (a), $q(z=f) = \dfrac{z_R f}{z_R - jf}$; $q(z=2f) = j\dfrac{f^2}{z_R - jf}$.

The expressions for the beam can be found by using the q parameters above and substituting in the general expression for the angular plane wave spectrum of a Gaussian, viz., $\tilde{E}_e(k_x, k_y) = \exp j(k_x{}^2 + k_y{}^2)q/2k_0$ and taking the inverse transform.

2. A Gaussian beam of width w and having wavefront with a radius of curvature R is normally incident on the interface between air and glass of refractive index n. Find the width and radius of curvature

(a) immediately after transmission through the interface,

(b) immediately upon reflection at the interface.

A2. The ABCD matrices for transmission and reflection at a plane interface are given by $\begin{pmatrix} 1 & 0 \\ 0 & 1/n \end{pmatrix}$ and $\begin{pmatrix} 1 & 0 \\ 0 & 1 \end{pmatrix}$, respectively. These ABCD matrices are derived for ray coordinates comprising the position and the angle of the ray (see for instance, Yariv and Yeh, Photonics, 6^{th} ed. Oxford, New York (2007). Given a certain q of the incident Gaussian beam, the transmitted beam will have a new q given by $q_{new} = \dfrac{Aq+B}{Cq+D}$. Hence for transmission, $q_{new} = nq$ or $\dfrac{1}{q_{new}} \equiv \dfrac{1}{R_{new}} - j\dfrac{2}{k_0 w_{new}^{\;2} n} = (1/n)\dfrac{1}{q} \equiv (1/n)\left(\dfrac{1}{R} - j\dfrac{2}{k_0 w^2}\right) = \dfrac{1}{nR} - j\dfrac{2}{k_0 w^2 n}$. Upon comparing, it readily follows that $R_{new} = nR;\; w_{new} = w$. For reflection, the values of the radius of curvature and the width are unchanged.

3. A Gaussian beam of waist w_0 of wavelength λ is incident on a slice of dielectric material of thickness L with a refractive index $n(x) = n_0 + \Delta n \cos Kx$ with $w_0 >> 2\pi / K$. Calculate the far-field diffraction pattern of the beam after transmission through the material

(a) assuming a thin sample i.e., $L << z_R$ where z_R is the Rayleigh range of the Gaussian beam, and normal incidence,

(b) assuming a thick sample $L > z_R$ and with $K^2 L\lambda >> 1$, and incidence at Bragg angle given by $\phi_B = \sin^{-1}(K\lambda / 4\pi)$.

A3. (a) Assume a Gaussian $E_e = \exp(-x^2/W^2)$ incident on a "thin" phase grating with refractive index $n(x) = n_0 + \Delta n \cos Kx$. Upon exit from the grating, the Gaussian beam acquires phase modulation and the field is given by $E_e \exp - jk_0 n(x)L = \exp(-x^2/W^2)\exp - jk_0(n_0 + \Delta n \cos Kx)L$, $k_0 = 2\pi/\lambda$. The far-field pattern is therefore proportional to the convolution of the Fourier transforms of $\exp(-x^2/W^2)$ and $\exp - jk_0 \Delta n L \cos Kx$ and with the spatial frequency replaced as $k_x = k_0 x / z$ The Fourier transform of $\exp(-x^2/W^2)$ is a Gaussian given as $\sqrt{\pi}W \exp - k_x^{\;2} W^2 / 4$. The the Fourier transform of $\exp - jk_0 \Delta n L \cos Kx$ is $\sum_{q=-\infty}^{\infty} J_q(k_0 \Delta n L)\delta(k_x - qK)$ where J_q is Bessel function of order q and the δ represents the delta function. So this resembles a series of delta functions located at $k_x = qK$ and having amplitudes equal to the Bessel functions. The convolution of the Gaussian and these delta functions will give a series of Gaussians centered at the locations of the delta functions, and with their peak amplitudes modulated according to the amplitudes of the Bessel functions. A typical simulation of this case is in the solution to Problem 4 below.

(b) Using Kogelnik's coupled wave theory, it follows that any plane wave of light not incident at exactly the Bragg angle onto a thick grating suffers a loss of diffraction efficiency. Since a Gaussian beam is comprised of angular plane wave components, this means that different plane waves which are not incident at the Bragg angle will suffer a loss of diffraction efficiency. In fact, the nature of the diffracted (and undiffracted) orders can be derived from the transfer functions of the respective orders, akin to what is done in acousto-optics (see, for instance, Refs. [4, 6]). For instance, the transfer function for the diffracted order is given as:

$$H_1(k_x) \propto -j\frac{k_0\Delta nL}{2}\frac{\sin\sqrt{(KL/2k_0)^2 k_x{}^2 + (k_0\Delta nL/2)^2}}{\sqrt{(KL/2k_0)^2 k_x{}^2 + (k_0\Delta nL/2)^2}}.$$

Multiplying the spectrum of the incident Gaussian with $H_1(k_x)$ and the transfer function $H(k_x)$ for propagation as given in this Chapter gives the spectrum of the Gaussian in the diffracted order, which is also proportional to the shape of the diffracted Gaussian in the far-field.

Typical plots of the Gaussian profiles for diffracted and undiffracted orders appear in Ref. [6].

4. Use the split step beam propagation technique to analyze propagation along z of a one-dimensional Gaussian beam of $w_0 = 100\lambda_0$ (λ_0 is the free-space wavelength) incident onto a grating made using a material of quiescent refractive index n_0. The grating has a thickness of $L = 100\lambda_0$ with a refractive index profile $n(x) = n_0 + \Delta n\,\mathrm{sgn}(\cos Kx)$, $K = 2\pi/\Lambda, \Lambda = 5\lambda_0$ and where sgn denotes the signum function. Assume $n_0 = 1.5, \Delta n = 0.00015$. Calculate the profile at the exit plane of the grating and in the far field. Repeat the problem for the case where the thickness of the grating is $L = 1000\lambda_0$ and characterize the differences between the two cases.

A4. Assume that the Gaussian beam is incident first on a sinusoidal grating given by $n(x) = n_0 + \Delta n[\cos Kx]$, for which the solutions for plane wave illumination for a thin grating are given as Bessel functions. The following sequence of figures show the far field diffraction pattern of the Gaussian diffracted by the sinusoidal grating. The "far field" is taken as 10 times the Rayleigh range of the incident Gaussian. The wavelength is taken as $0.5\mu m$.

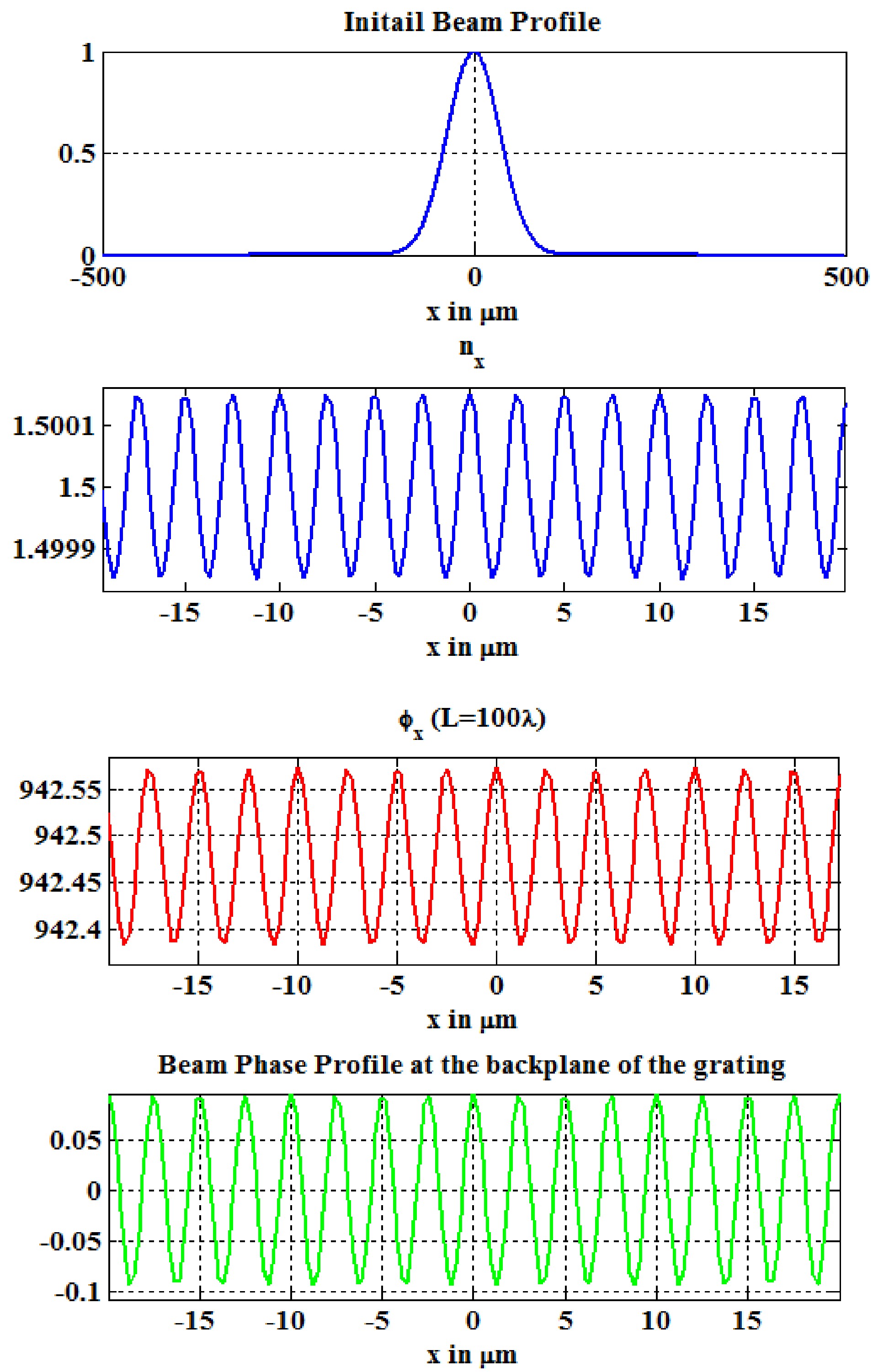
Initail Beam Profile
1
0.5
0
-500
0
500
x in µm
n_x
1.5001
1.5
1.4999
-15
-10
-5
0
5
10
15
x in µm
ϕ_x (L=100λ)
942.55
942.5
942.45
942.4
-15
-10
-5
0
5
10
15
x in µm
Beam Phase Profile at the backplane of the grating
0.05
0
-0.05
-0.1
-15
-10
-5
0
5
10
15
x in µm

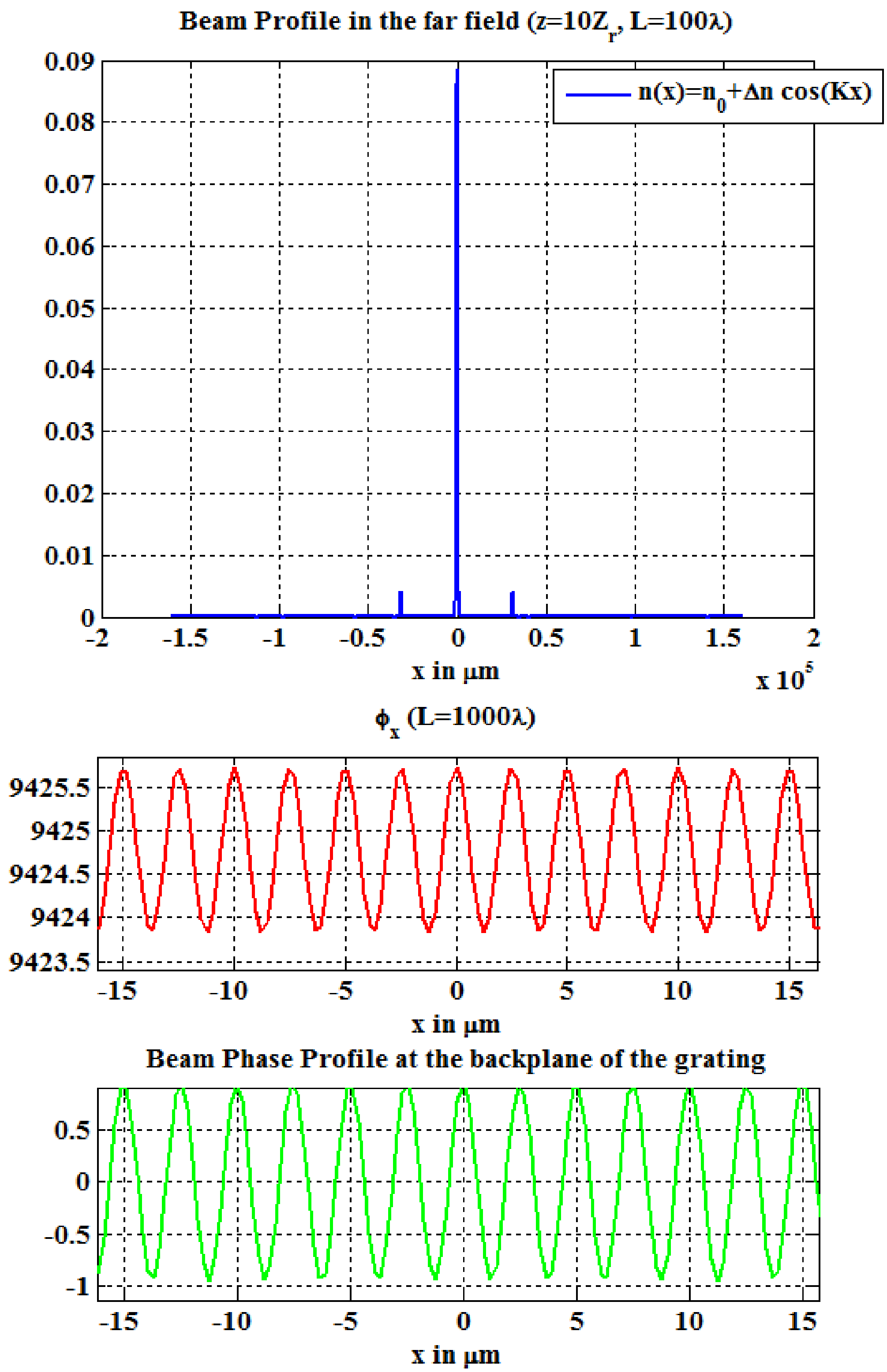
Beam Profile in the far field (z=10Z_r, L=100λ)
n(x)=n_0+Δn cos(Kx)
x in μm
x 10^5
ϕ_x (L=1000λ)
x in μm
Beam Phase Profile at the backplane of the grating
x in μm

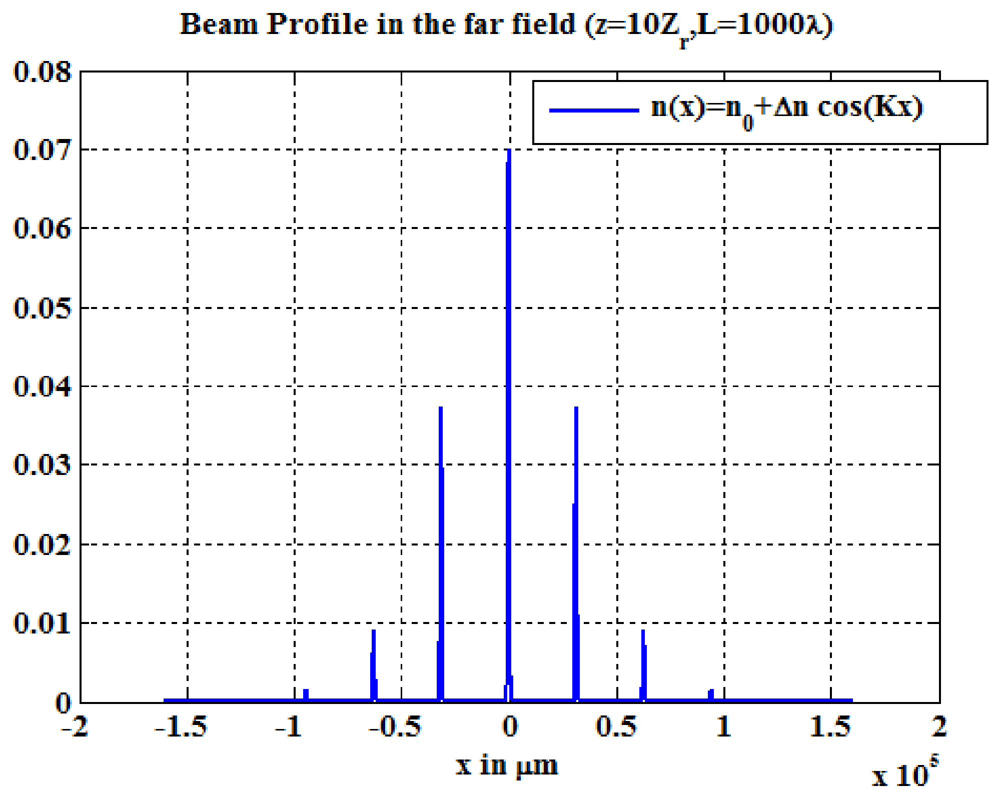

The procedure is now repeated for the grating $n(x) = n_0 + \Delta n \,\mathrm{sgn}[\cos Kx]$. The results are shown below. Note the appearance of more orders due to the Fourier content of the signum function.

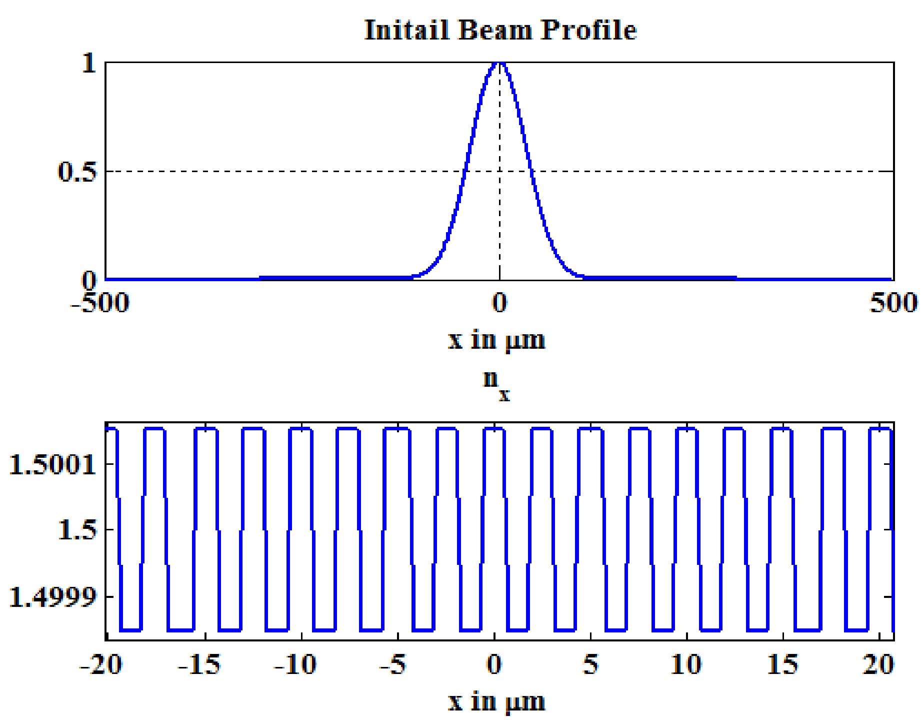

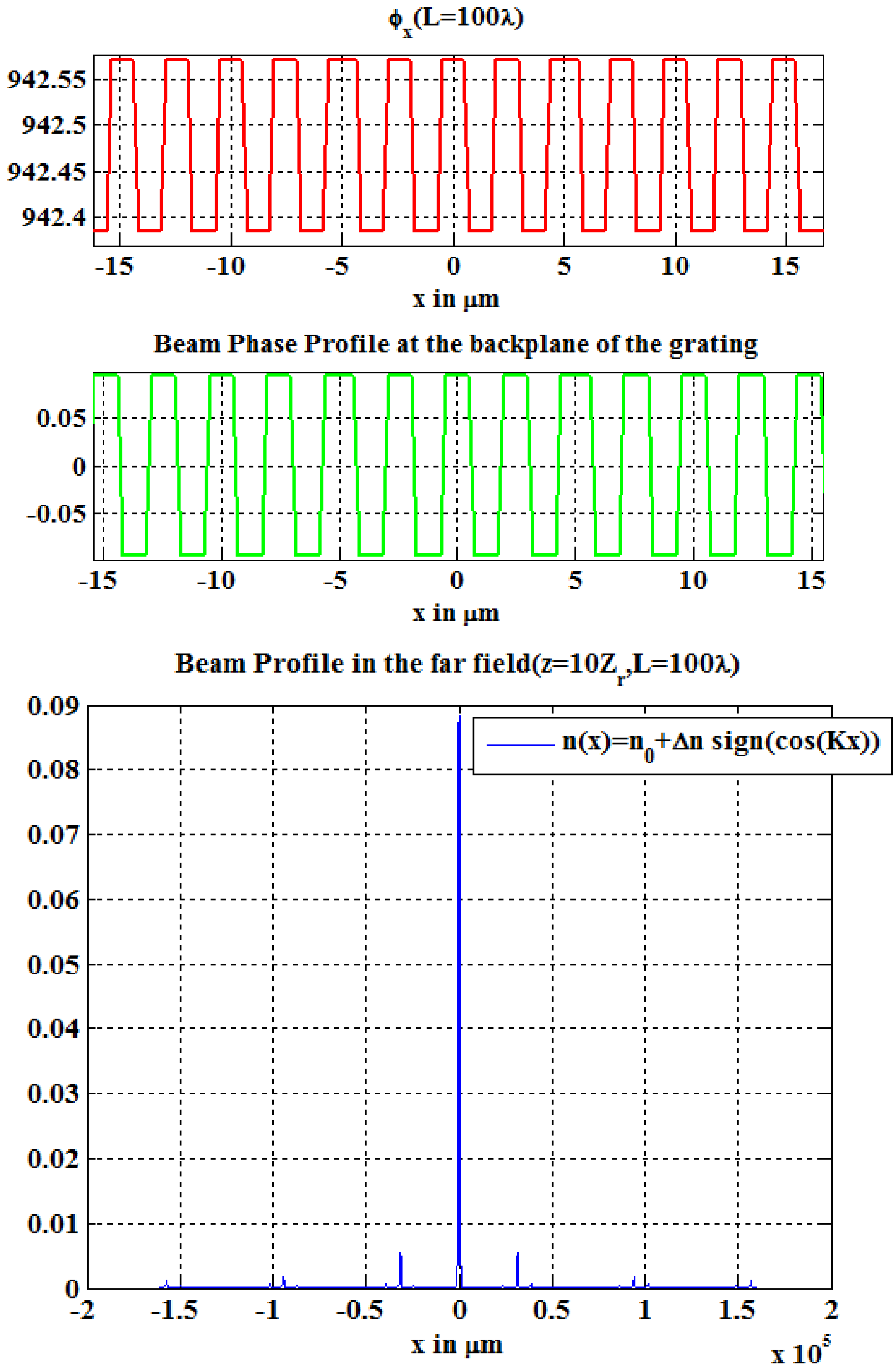

ϕx(L=100λ)
942.55
942.5
942.45
942.4
-15 -10 -5 0 5 10 15
x in μm
Beam Phase Profile at the backplane of the grating
0.05
0
-0.05
-15 -10 -5 0 5 10 15
x in μm
Beam Profile in the far field(z=10Zr,L=100λ)
n(x)=n0+Δn sign(cos(Kx))
0.09 0.08 0.07 0.06 0.05 0.04 0.03 0.02 0.01 0
-2 -1.5 -1 -0.5 0 0.5 1 1.5 2
x in μm
x 10^5

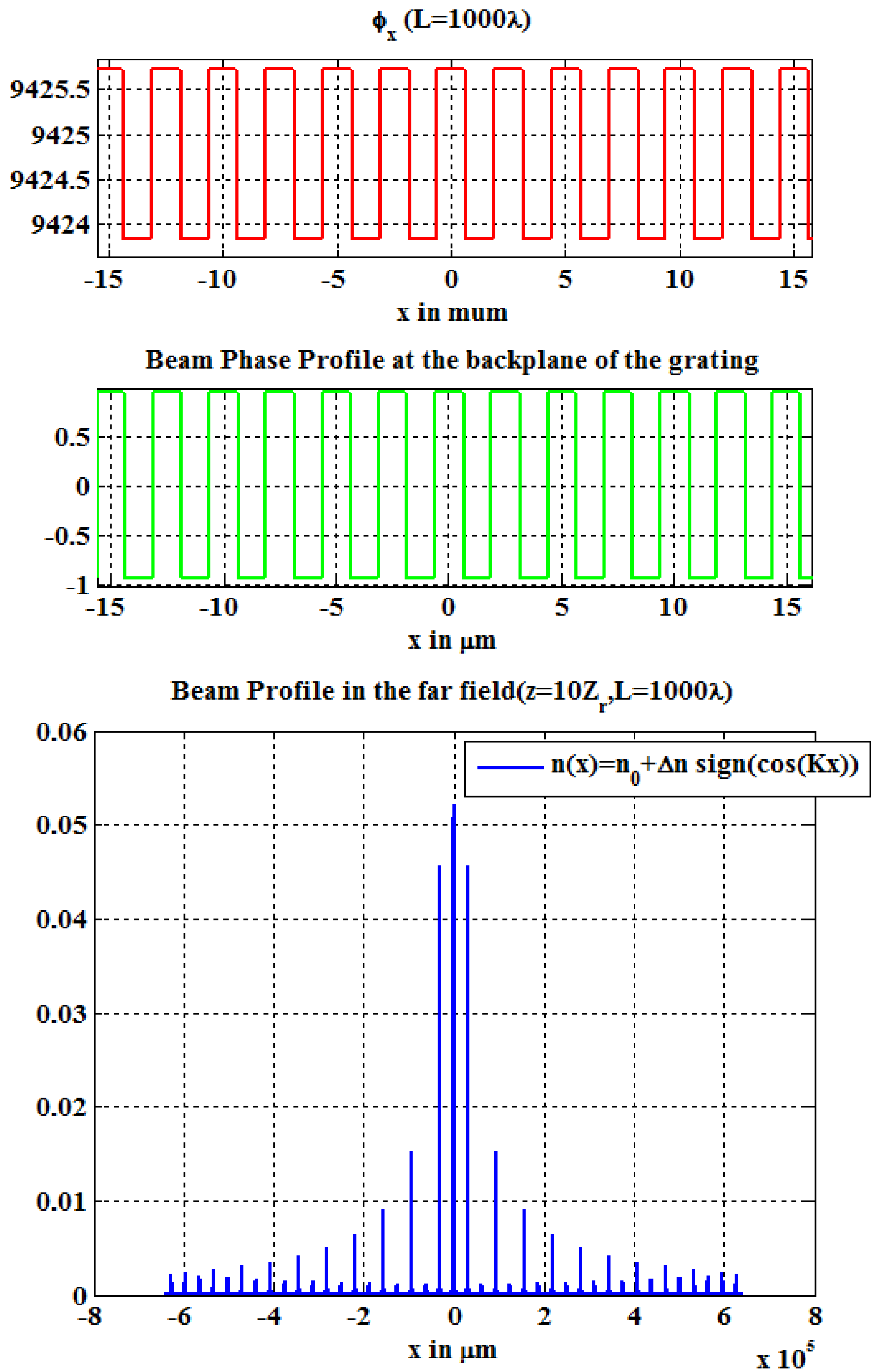

φx (L=1000λ)
9425.5
9425
9424.5
9424
-15
-10
-5
0
5
10
15
x in mum
Beam Phase Profile at the backplane of the grating
0.5
0
-0.5
-1
x in µm
Beam Profile in the far field(z=10Zr,L=1000λ)
n(x)=n0+Δn sign(cos(Kx))
0.06
0.05
0.04
0.03
0.02
0.01
-8
-6
-4
-2
2
4
6
8
x in µm
x 10^5

5. Analyze the propagation of a Gaussian beam of waist $w_0 = 100\lambda_0$ through a material of thickness $L = 100\lambda_0$ having a refractive index profile $n(x) = n_0 + \alpha(x/w_0), |x| < 5w_0$. Let $n_0 = 1.5, \alpha = 0.015$. Determine the far-field intensity profile. You may use analytical techniques and/or the beam propagation method.

A5. The wavelength is taken as $0.5\mu m$. The far field is 100 times the Rayleigh range of the Gaussian beam. The shift of the center in the far field arises from the linear phase applied to the Gaussian beam.

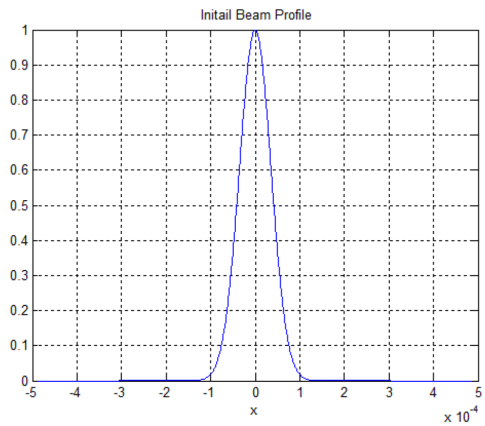

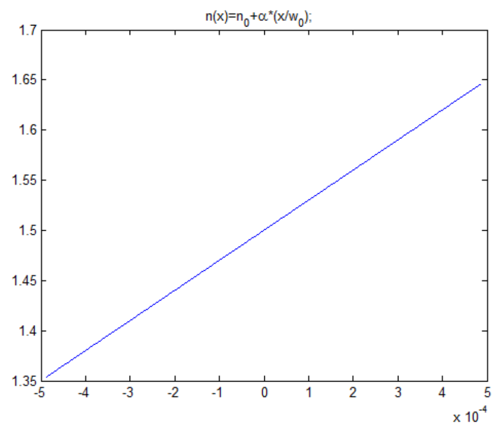

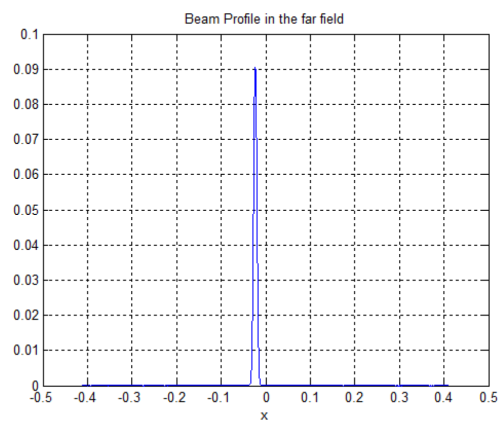

6. A Gaussian beam of waist $w_0 = 100\lambda_0$ symmetric about $x = 0$ is incident from air onto a nonlinear material slab of thickness $L = 100\lambda_0$ and of refractive index $n(x) = n_0 + n_2 I(x),\ n_0 = 1$ where $I(x)$ is the intensity of the Gaussian beam. Assume that a knife edge is present at $z = 0$. Use the split step method to determine the far field profile. At $z = 0^-$, assume $n_2 I(0) = 10^{-4}$.

A6. The wavelength is taken as $0.5\mu m$. The far field is taken as 10 times the Rayleigh range of the Gaussian beam.

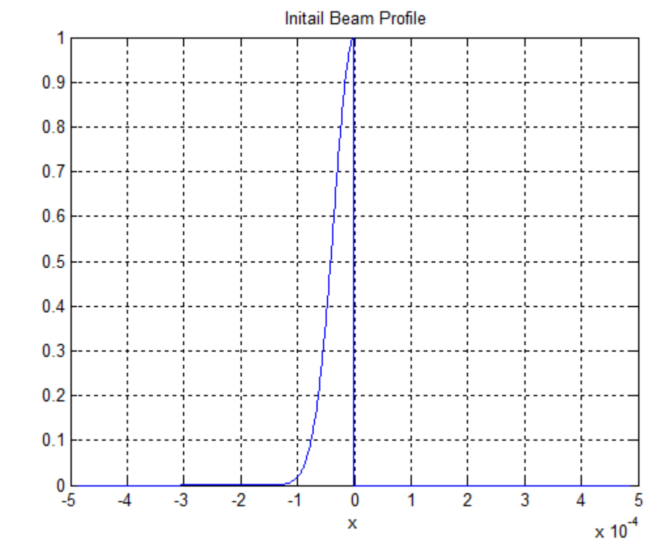
Initail Beam Profile
x
x 10^-4

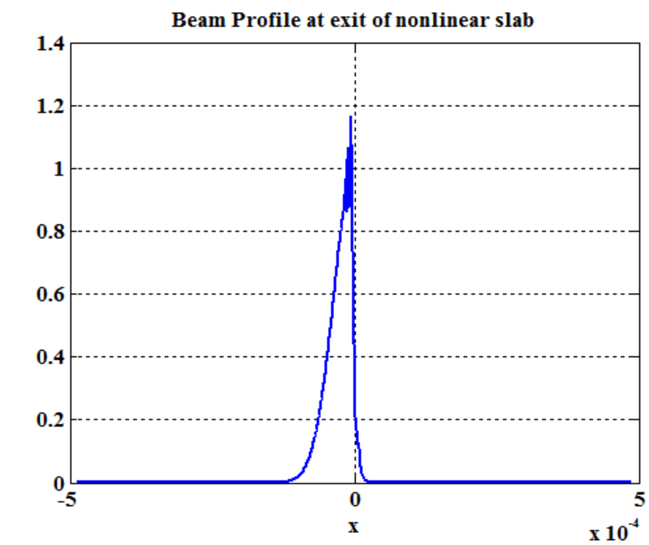
Beam Profile at exit of nonlinear slab
x
x 10^-4

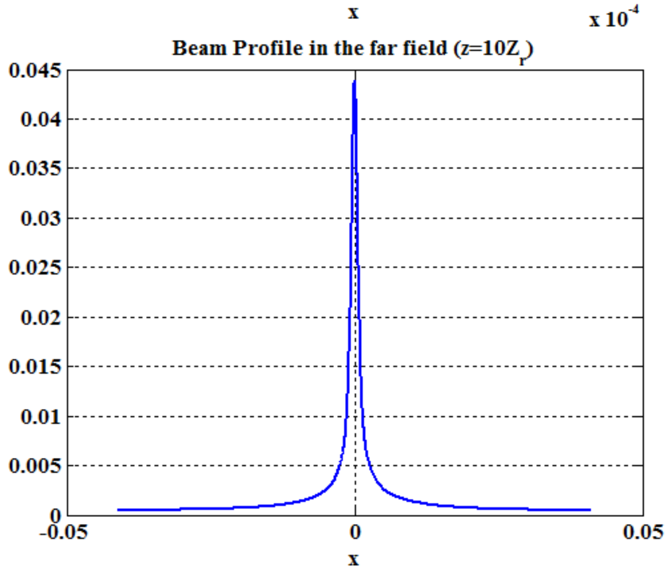
Beam Profile in the far field (z=10Z_r)
x

7. The paraxial nonlinear Schrodinger equation can be written as $j\partial u/\partial z + \frac{1}{r^{D-1}}\frac{\partial}{\partial r}(r^{D-1}\partial u/\partial r) + f(|u|^2)u = 0$ where D represents the dimension of the problem. For the case $D = 2$ (cylindrical symmetry) and $f(|u|^2) = |u|^2$ (a) use the Hankel transform technique to numerically plot representative beam on-axis amplitudes during propagation all the way to near the self-focusing point for an initial profile $u_0 = 4e^{-r^2/2}$; (b) repeat part (a) for the case when, as in the text, a fixed and adaptive nonparaxiality parameter has been included.

A7. See the text for the figures (Fig. 2.13), and Ref. [22].

8. (a) Plot the on-axis amplitudes as a function of propagation distance for the case of the paraxial nonlinear Schrodinger equation with cylindrical symmetry but for an initial profile $u_0 = 4e^{-r^2}$. (b) Repeat part (a) for the case when, as in the text, a fixed and adaptive nonparaxiality parameter has been included [22].

A8. See Ref. [22] and Fig. 4 therein.

9. In the paraxial nonlinear Schrodinger equation $j\partial u/\partial z + \frac{1}{r^{D-1}}\frac{\partial}{\partial r}(r^{D-1}\partial u/\partial r) + f(|u|^2)u = 0$, setting $D = 3$ implies spherical symmetry. Assume $f(|u|^2) = \frac{|u|^2}{1+\mu|u|^2}$. Use a change of variable $u = r^{-l}v; l = 1/2$ to change the radial operator from spherical to cylindrical coordinates. Thereafter, by using a suitable initial condition, sketch typical profiles of the spherically symmetric shapes that are stable during propagation. For hints and details of the Hankel transform to be used, readers are referred to Nehmetallah and Banerjee [46].

A9. If use the spherical symmetry of the field distribution and introduce the radial variable $r = \left(x^2 + y^2 + \tau^2\right)^{1/2}$, the paraxial nonlinear Schrodinger equation can be written as

$$j\frac{\partial u}{\partial z} + \frac{1}{r^{D-1}}\frac{\partial}{\partial r}\left(r^{D-1}\frac{\partial u}{\partial r}\right) + f\left(|u|^2\right)u = 0, \tag{1}$$

where D is 3, $f\left(|u|^2\right) = \frac{|u|^2}{1+\mu|u|^2} \approx |u|^2 - \mu|u|^4$. Let us assume the initial profile to be $u = A(z)\exp\left[-\left(1 + jb(z)\right)\frac{r^2}{2w^2(z)} + j\phi(z)\right]$ where *A(z)* is the amplitude, *w(z)* is the beam radius, *b(z)* is the wave front curvature, and $\phi(z)$ is the phase as unknown functions of the propagation distance *z*.

The second term in Eq. (1) becomes

$$\left(\frac{\partial^2}{\partial r^2} + \frac{D-1}{r}\frac{\partial}{\partial r}\right)u. \tag{2}$$

The Hankel transform or Fourier Bessel technique can not apply directly to this operator in the case when *D=3*, so we have to transform the operator from spherical coordinates to cylindrical ones by letting $u(r,z)=r^{-l}v(r,z)$, where *l* is the order of the Fourier Bessel or Hankel transform. Relation (2) becomes $\left(\frac{\partial^2}{\partial r^2}+\frac{1}{r}\frac{\partial}{\partial r}-\frac{l^2}{r^2}\right)v \xrightarrow{AFHSS} -4\pi^2\rho^2 v_{\mathcal{H}}(\rho,z)$, where $v_{\mathcal{H}}(\rho,z)=\mathcal{H}_\ell[v(r,z)]= \mathcal{H}_\ell[r^l u(r,z)] \Rightarrow u(r,z)=r^{-l}\mathcal{H}_\ell[v_{\mathcal{H}}(\rho,z)]$, with $l=0,\ 1/2$ in the case of the cylindrical and spherical Fourier Bessel transform pair respectively where they are related to each other by:

$$u(r,z)=\int_0^\infty u_{\mathcal{H}}(\rho,z)j_{l-1/2}(\rho r)\rho^{l+3/2}d\rho=\sqrt{\frac{\pi}{2}}r^{-l}\int_0^\infty \rho^{l+1}u_{\mathcal{H}}(\rho,z)J_l(\rho r)d\rho, \tag{3}$$

$$u_{\mathcal{H}}(\rho,z)=\frac{2}{\pi}\int_0^\infty u(r,z)j_{l-1/2}(\rho r)r^{l+3/2}dr=\sqrt{\frac{2}{\pi}}\rho^{-l}\int_0^\infty r^{l+1}u(r,z)J_l(\rho r)dr, \tag{4}$$

where $j_l(x)=(-x)^l\left(\frac{1}{x}\frac{d}{dx}\right)^l\frac{sin(x)}{x}=\sqrt{\frac{\pi}{2x}}J_{l+1/2}(x)$ is the l^{th} order spherical Bessel function. The above transform pair is solved by the l^{th} order finite Hankel Transform method. The algorithm is shown in the flowchart below. Simulation results using the ASFBSS method appear in Ref. [46].

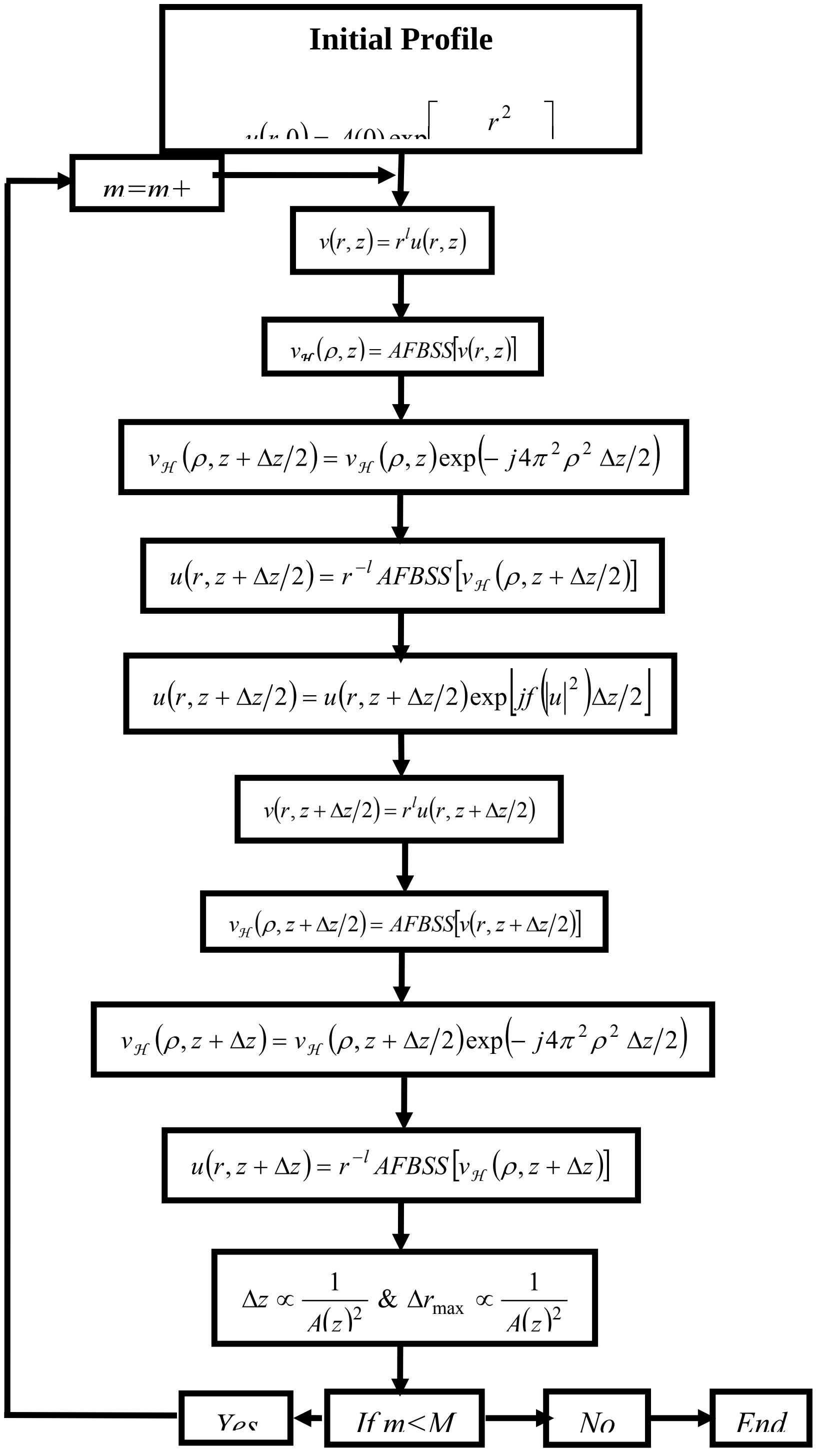

10. Derive representative *z*-scan graphs for the case where the (thin) lens to be characterized is a linear lens with a fixed focal length f which is independent of the intensity of the light (but may depend on other parameters such as applied voltage across the sample lens as in a electro-optic lens. In this case, show that the *z*-derivative of the on-axis intensity is similar to the traditional *z*-scan signature of a nonlinear induced lens.

A10. Assume a typical z-scan setup as shown in the figure below, where the output beam from a laser is first expanded by a lens of focal length f_1 and then focused to a waist w_0 with a second lens of focal length f_2. The sample under test is scanned through a distance Δz about the location of this waist.

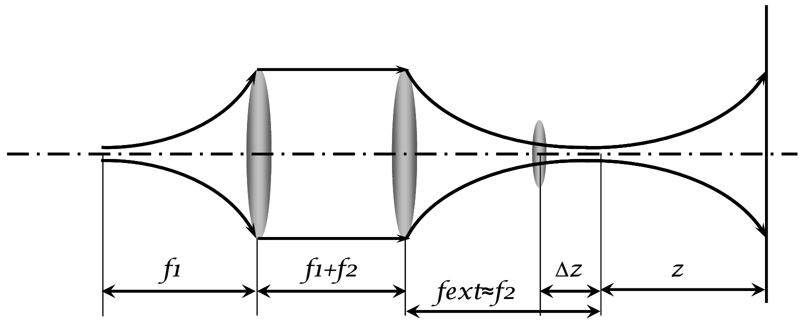

The Gaussian optical field distribution at this plane which is incident on the test lens of focal length f can be expressed as

$$E(x,y)=\frac{q_0}{q_0+\Delta z}\exp\left(-\frac{j\left(x^2+y^2\right)k_0}{2\left(q_0+\Delta z\right)}\right), \tag{1}$$

where q_0 $\left(= jz_R = jk_o w_0^{\ 2}/2\right)$ is the q-parameter of the beam at the focus of the second external lens and z_R is the Rayleigh range. Hence, the optical field distribution on the observation plane a distance $Z >> \Delta z > z_R$ from the waist location can be expressed as

$$E(x,y,Z)=\frac{jk_0}{2\pi Z}\iint \Im(x',y')\times\exp\left(-\frac{jk_0}{2Z}\left[\left(x-x'\right)^2+\left(y-y'\right)^2\right]\right)dx'dy', \tag{2}$$

with

$$\Im(x,y)=E(x,y)T_f(x,y), \tag{3}$$

where the Gaussian field distribution $E(x,y)$ given in Eq. (1), and the lens transmission function

$$T_f(x',y')=\exp\left(\frac{j\left(x^2+y^2\right)k_0}{2f}\right). \tag{4}$$

The on-axis transmittance on the observation plane is given by

$$I(0,0,Z)\propto E(0,0,Z)E^*(0,0,Z), \tag{5}$$

which can be reexpressed, after some algebra, as

$$I(0,0,Z)\propto\frac{k_0^2}{4\pi^2Z^2f^2}\frac{\left|q_0\right|^2}{\left|q_0\right|^2+\left(\Delta z\right)^2}\left|q_z\right|^2\left\{1+\exp\left(\frac{-k_0r_0^2b}{\left|q_z\right|^2}\right)-2\exp\left(\frac{-k_0r_0^2b}{2\left|q_z\right|^2}\right)\cos\left(\frac{k_0r_0^2a}{2\left|q_z\right|^2}\right)\right\}, \tag{6}$$

$$\frac{1}{q_z}=\frac{1}{q_0+\Delta z}+\frac{1}{Z}-\frac{1}{f}, \tag{7}$$

$$a=\mathrm{Re}\left(q_z\right),\ b=\mathrm{Im}\left(q_z\right). \tag{8}$$

Simulated Z-scan plots for normalized on-axis z-scan intensity, obtained for test lens focal length values that varies between 2-20 *mm* in 2 *mm* increments, detected 1m away from the focus of the test lens, are shown in the figure below for a probing beam of waist size 50 μm. Also shown is the derivative w.r.t. Z of the z-scan plots. This graph is akin to the standard z-scan plots of a nonlinear Kerr-type material.

For further detail on z-scans of linear lenses and their application to measurements of focal lengths of electrooptics PLZT lenses, the reader is referred to Y. Abdelaziez and P.P. Banerjee, "Modeling and characterization of PLZT adaptive microlenses", **Journal of Microlithography, Microfabrication, and Microsystems** vol. **7**, pp. 013011:1-10 (2008).

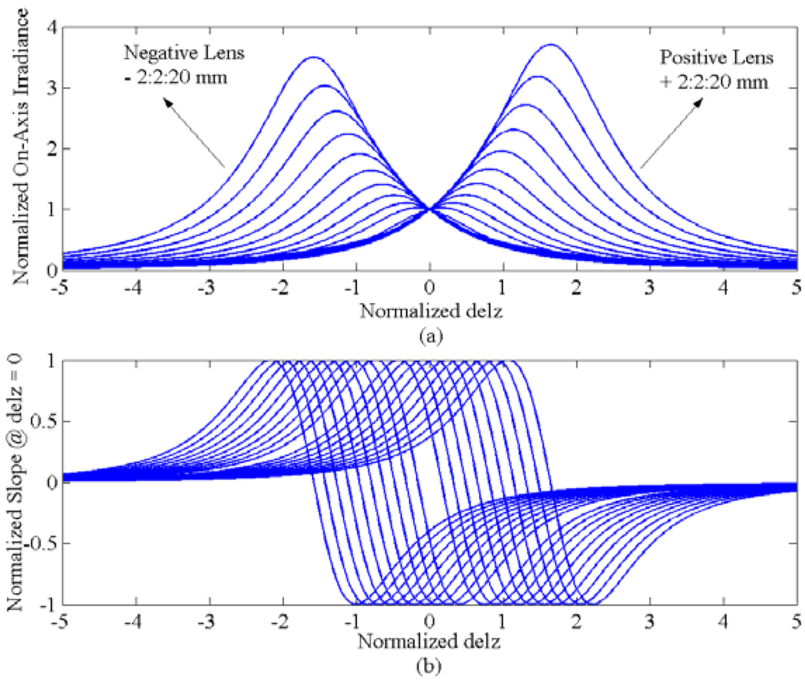

11. Derive representative *z*-scan graphs for the case when the sample under test has a induced refractive index as in a diffusion dominated photorefractive material, and given by $\Delta n \propto \partial I / \partial x$, assuming one transverse dimension. Assuming thin sample, for simplicity. Show that the nature of the z-scan graph is an even function of the displacement from the back focal plane of the external lens. For hints and details, readers are referred to Noginov *et al*. [47].

A11. Assume that the incoming beam is a Gaussian of the form $A\exp(-r^2/w_0^2)$. The phase of the optical field immediately behind the sample is, in this case, proportional to the spatial derivative of the intensity profile:

$$\Delta\Phi(r,z) = \Delta\Phi_o(z)\frac{\partial}{\partial r}\exp\left[-\frac{2r^2}{w^2(z)}\right] , \tag{1}$$

where $\Delta\Phi_o(z)$ depends on the peak beam amplitude A and photorefractive parameters. At the focus ($z = 0$), the complex optical field can be written as

$$E(r,0) = E(0,0)\exp\left(\frac{-r^2}{w_o^2} - j\frac{\partial}{\partial r}\Delta\Phi(r,0)\right) \tag{2}$$

As in the analysis of the z-scan for Kerr type nonlinearities, expanding the Gaussian components of these complex phase shift results in the series

$$E(r,0) = E(0,0) \sum_{m=0}^{\infty} \frac{[-jb(r)]^m}{m!} \exp\left(\frac{-r^2}{w_m^2(0)}\right) \tag{3}$$

where $b(r) = -4r / w^2(0)$ is a function of radial variation. The optical field immediately behind the thin nonlinear sample placed a distance z from focus can be written as

$$E(r,z) = E_{inc}(r,z) \sum_{m=0}^{\infty} \frac{[-j\Delta\Phi_o(z)]^m}{m!} \frac{[-4r]^m}{[w^2(z)]^m} \exp\left(\frac{-r^2}{w_m^2(z)}\right)$$

$$= E_0 \frac{w_o}{w(z)} \exp(-ikr^2 / 2R(z)) \sum_{m=0}^{\infty} \frac{[-j\Delta\Phi_o(z)]^m}{m!} \frac{[-4r]^m}{[w^2(z)]^m} \exp\left(\frac{-r^2}{w_m^2(z)}\right) \tag{4}$$

where all z-dependent values are also measured with respect to the back focal plane of the external lens, $w^2(z)$, $R(z)$ are respectively the width and radius of curvature of the radially symmetric Gaussian beam for arbitrary scan distance z, as mentioned above, $w_m^2(z) = w^2(z)/(2m+1)$, and $\Delta\Phi_o(z) = \Delta\Phi_o / (1+(z/z_R)^2)^{1/2}$, z_R denotes the Rayleigh length corresponding to w_o.

The far-field optical field pattern for any sample position z is

$$E_{ff}(k_r, z) = \int_0^{\infty} r\, E(r,z)\, J_0(k_r r)\, dr , \tag{5}$$

where k_r has the connotation of a spatial transverse variable according to $k_r = k_0 r / z_{ff}$, where z_{ff} denotes the distance to the far-field after the sample. Terms in the resulting series can be evaluated using

$$\int_0^{\infty} x^u \exp(-\alpha x^2) J_v(\beta x) dx = \frac{\beta^v \Gamma((u+v+1)/2)}{2^{v+1} \alpha^{(u+v+1)/2} \Gamma(v+1)} F_1^1\left(\frac{u+v+1}{2}; v+1; -\beta^2/4\alpha\right) \tag{6}$$

where Γ and F_1^1 are the gamma function and confluent hypergeometric function respectively. Using the properties of a Gaussian beam, the normalized intensity at any point in the observation plane $I(k_r,z)$ is given by

$$I(k_r, z, \Delta\Phi_o) = \frac{\left|E(k_r, z, \Delta\Phi_o(z)\right|^2}{\left|E(k_r = 0, z, \Delta\Phi_o(z = 0)\right|^2} . \tag{7}$$

The z-scan plots, drawn based on the theory above can be found in Ref. [47]. These show that derivative nonlinearity gives rise to an "even" z-scan graph centered around the location of the back focal plane of the external lens (z=0), contrary to the Kerr-type nonlinearity case, where the z-scan graph is an odd function of the scan length.

12. If the induced refractive index of a material is proportional to the gradient of the intensity, show how this effect may be used in image processing applications such as edge enhancement of an image. For hints, readers are referred to Banerjee *et al*. [48].

A12. The key to this is to realize that if $\Delta n = C\partial I/\partial x$, then for a thin sample and weak nonlinearity, the optical output for an incident optical field E_e is $E_e \exp - jk_0 \Delta n L = E_e \exp - jk_0 LC\partial I/\partial x \approx E_e[1 - jk_0 LC\partial I/\partial x]$. The last term is proportional to the derivative of the intensity, which amounts to a high pass filtering of the intensity pattern. This yields the edge enhancement of the image, since edges contain higher spatial frequencies.

A way to realize this is using a two-wave coupling arrangement as in simultaneous holographic recording and readout such that in the material, the pump beam interacts with the signal beam which is proportional to the Fourier transform of the object, as shown in the figure.

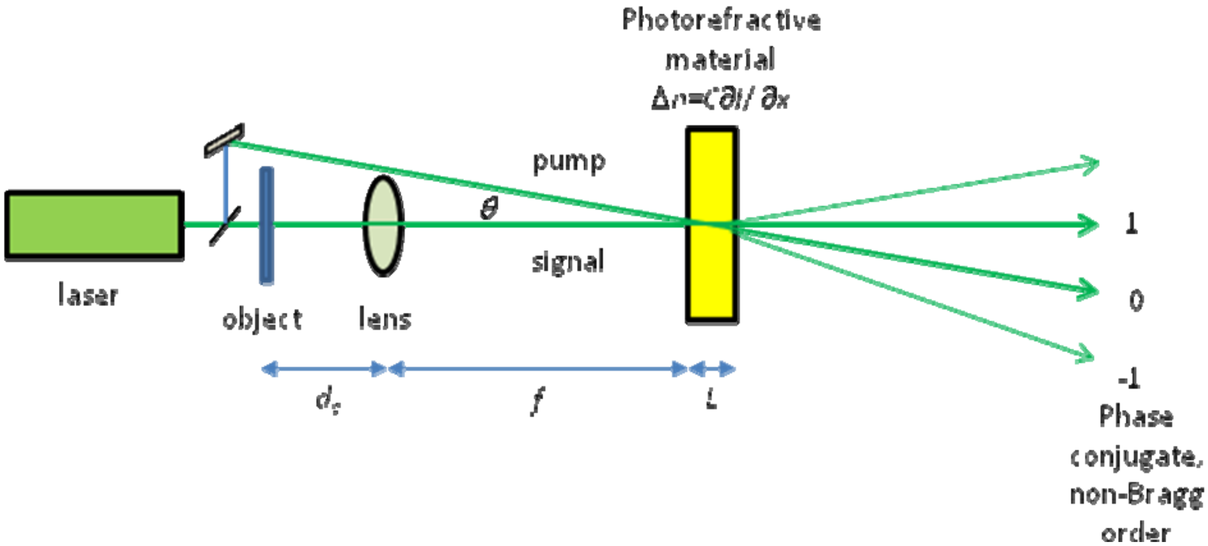

Suppose that the pump beam is denoted as E_{ep} and the signal beam as E_{es} at the input face of the material, then $\Delta n = C\partial I/\partial x = C\partial \left|E_{ep} + E_{es}\right|^2/\partial x$. When this phase grating is simultaneously read out by the pump beam, the optical field immediately behind the material is given by $E_{ep}[1 - k_0 LC\partial \left|E_{ep} + E_{es}\right|^2/\partial x]$, which gives rise to higher order (-1order) diffraction, in addition to the conventional 0^{th} and 1^{st} orders. This higher order diffraction also contains the phase conjugate of the object, which is of interest to us here. For instance, let the pump be denoted as $E_{ep} \propto \exp - jk_0 x\theta$ where $\theta << 1$represents the angle between the pump and the signal. The signal beam incident on the material is proportional to the spatial Fourier transform of the object and given by $E_{es} \propto \exp\{-jk_0[1 - d_o/f]x^2/2f\} \bullet T(k_0 x/f)$where $T(k_x) = \Im_x[t(x)]$, and where d_o is the distance of the object $t(x)$ in front of the Fourier transforming lens of focal length f. Then the -1 order propagating at 2θ contains a term proportional to $j[1 - d_o/f]k_0 x/f\} \bullet T^*(k_0 x/f)\exp jk_0[1 - d_o/f]x^2$. Now using Fresnel propagation, it can be shown that at a distance $z_i = f/[1 - d_o/f]$behind the material, the optical field has a component proportional to $\partial t^*/\partial x$, which is the edge enhanced spatial conjugation of the object. For pictures of edge enhanced objects, the reader is referred to Ref. [48].